Physics Letters B 730 (2014) 59–62

Contents lists available at ScienceDirect

Physics Letters B

www.elsevier.com/locate/physletb

Testing the Bardeen metric with the black hole candidate in Cygnus X-1

Cosimo Bambi

Center for Field Theory and Particle Physics & Department of Physics, Fudan University, 200433 Shanghai, China

ARTICLE INFO

Article history:
Received 24 August 2013
Received in revised form 19 January 2014
Accepted 19 January 2014
Available online 22 January 2014
Editor: S. Dodelson

ABSTRACT

In general, it is very difficult to test the Kerr-nature of an astrophysical black hole candidate, because it is not possible to have independent measurements of both the spin parameter a_* and possible deviations from the Kerr solution. Non-Kerr objects may indeed look like Kerr black holes with different spin. However, it is much more difficult to mimic an extremal Kerr black hole. The black hole candidate in Cygnus X-1 has the features of a near extremal Kerr black hole, and it is therefore a good object to test the Kerr black hole paradigm. The 3σ-bounds $a_* > 0.95$ and $a_* > 0.983$ reported in the literature and valid in the Kerr spacetime become, respectively, $a_* > 0.78$ and $|g/M| < 0.41$, and $a_* > 0.89$ and $|g/M| < 0.28$ in the Bardeen metric, where g is the Bardeen charge of the black hole.

Astrophysical black hole (BH) candidates are supposed to be the Kerr BHs predicted in general relativity, but the actual nature of these objects has still to be verified [1]. At present, there are only two relatively robust techniques capable of probing the geometry of the space–time around BH candidates; that is, the continuum-fitting method [2] and the analysis of the Kα iron line [3]. Under the Kerr BH paradigm, these techniques can provide an estimate of the spin parameter $a_* = J/M^2$, where M and J are, respectively, the BH mass and spin angular momentum.[1] Both the continuum-fitting method and the iron line analysis have been extended to non-Kerr spacetimes to test the nature of BH candidates [4,5]. However, in general it is only possible to constrain some combination between the spin and possible deviations from the Kerr solution: the spectrum of non-Kerr objects can be very similar to the one of Kerr BHs with a different spin parameter.

While a number of very exotic metrics can already be ruled out by current observations with these techniques [6], some more theoretically motivated non-Kerr metrics are very difficult to test and the combination of the continuum-fitting method and the iron line analysis cannot solve the degeneracy between the spin and the deformation parameters [7]. The difficulty to constrain deviations from the Kerr metric independently of the measurement of the spin is common to other (potentially more sophisticated) approaches, like the observation of quasi-periodic oscillations [8] and of the X-ray polarization [9]. This problem might be fixed in the future, at least partially, by combining one of the techniques above with the estimate of jet power [10] or the measurement of the BH shadow [11]. However, the observational features of near extremal Kerr black holes are peculiar, and therefore the observation of a BH candidate that looks like a near extremal Kerr BH can constrain the nature of these objects.

While the analysis of the iron line profile is potentially more powerful, the continuum-fitting method is based on more solid physics, the uncertainty on the final measurement is more reliable, and therefore this technique is at present more suitable to derive conservative but robust bounds. It is based on the study of the soft X-ray component of stellar-mass BH candidates, which is interpreted as the thermal spectrum of a geometrically thin and optically thick accretion disk. Among the BH candidates studied with the continuum-fitting method, there are two objects that look like near extremal Kerr BHs: GRS 1915+105 [12] and Cygnus X-1 [13,14]. Studies of the iron line analysis support this conclusion [15] (but see Ref. [16], whose discrepancy is probably due to the improper data state — not high/soft state — and the improper usage in the continuum model in extracting the skewed iron line profile [13]). GRS 1915+105 is a very peculiar source, whose data are difficult to interpret, and the measurement reported in Ref. [12] is based on the assumption that the jet observed in this source is perpendicular to the accretion disk, which is at least questionable. The studies in Refs. [13,14] of Cygnus X-1 are more recent and the results may be thought to be more robust. Under the assumption that the geometry of the spacetime around this object is described by the Kerr metric, the 3σ-bound on the spin parameter of the BH candidate in Cygnus X-1 is found to be $a_* > 0.95$ in [13] and $a_* > 0.983$ in [14].

E-mail address: bambi@fudan.edu.cn.

[1] Throughout the Letter, I use units in which $G_N = c = 1$, unless stated otherwise.

http://dx.doi.org/10.1016/j.physletb.2014.01.037

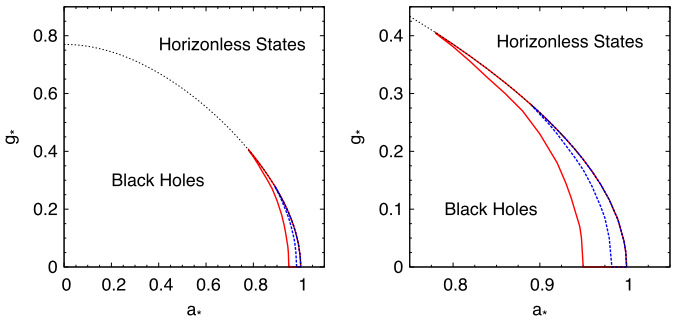

Fig. 1. Spin parameter-deformation parameter plane of the Bardeen metric. The thin black dashed line separates BHs from configurations without an event horizon (i.e. $\Delta = r^2 - 2mr + a^2 = 0$ has no real roots). The thick red solid line and the thick blue dashed line are the boundaries of the allowed regions for the BH candidate in Cygnus X-1 inferred, respectively, from the 3σ-bound obtained in the Kerr metric $a_* > 0.95$ in Ref. [13] and $a_* > 0.983$ in Ref. [14]. The right panel is an enlargement of the left panel. See the text for more details. (For interpretation of the references to color in this figure legend, the reader is referred to the web version of this article.)

The aim of this Letter is to test the Bardeen metric, which describes the spacetime of a singularity-free BH and can be formally obtained by coupling Einstein's gravity to a non-linear electrodynamics field [17]. In Boyer–Lindquist coordinates, the metric of the rotating solution is equivalent to the Kerr metric with the mass M replaced by the function m, given by [18]

$$M \to m = M\left(\frac{r^2}{r^2+g^2}\right)^{3/2}, \tag{1}$$

where r is the radial coordinate and g is the magnetic charge of the non-linear electrodynamics field (or simply the deformation measuring the deviations from the Kerr metric). As g has the same dimension as M, in analogy with the dimensionless spin parameter a_* it is convenient to introduce the dimensionless deformation parameter $g_* = g/M$. Let us note that $m \to M$ at large radii. The radius of the event horizon, which is given by the largest root of $\Delta = r^2 - 2Mr + a^2 = 0$ (where $a = J/M$ is the specific spin angular momentum) in the Kerr spacetime, is now the largest root of $\Delta = r^2 - 2mr + a^2 = 0$. Bardeen BHs exist only below a critical spin parameter $a_*^{\rm c}$, which depends on the value of g_* and reduces to the Kerr one $a_*^{\rm c} = 1$ for $g_* = 0$, while for $a_* > a_*^{\rm c}$ there is no horizon and the metric can be thought to describe the gravitational field of a configuration of exotic matter (see Fig. 1). The Bardeen metric can be seen as the prototype of a large class of non-Kerr BH metrics, in which the metric tensor in Boyer–Lindquist coordinates has the same expression of the Kerr one with M replaced by a mass function $m(r)$ that depends only on the radial coordinate r and that reduces to M as $r \to \infty$ [18]. This class of metrics is particularly difficult to test, because the corresponding disk's thermal spectrum and iron line profile are extremely similar to the one corresponding to a Kerr BH with different spin [7].

The standard procedure to test the Bardeen metric with the X-ray data of the BH candidate in Cygnus X-1 would be to repeat the studies of Refs. [13,14] with the Kerr background replaced by the Bardeen one. This would require a detailed analysis to include a large number of astrophysical effects and would be very time consuming. However, we can arrive at the same result with a much faster approach. The key-point is that the thermal spectrum of a thin disk can be used to fit only one parameter of the background geometry. If we assume the Kerr metric, we can infer the BH spin parameter a_*. If we relax the Kerr BH hypothesis, we can measure some combination of the spin parameter and of possible deviations from the Kerr solution. As shown in Fig. 2, the disk's thermal spectrum of a Bardeen BH with specific values of a_* and g_* is practically indistinguishable from the one of a Kerr BH with spin $\tilde{a}_*$ ($\neq a_*$). Bardeen BHs with the same g_* and spin parameter higher (lower) than a_* look like Kerr BHs with spin parameter higher (lower) than $\tilde{a}_*$. Since here the goal is to test the background metric around the BH candidate in Cygnus X-1, we do not need to repeat the analysis of Refs. [13,14] with the Bardeen background, but we can simply translate the Kerr measurements $a_* > 0.95$ and $a_* > 0.983$ to a bound on a_* and g_* by comparing the theoretical predictions of disk's thermal spectrum around Kerr and Bardeen BHs.

Calculation method. The calculations of the thermal spectrum of a geometrically thin and optically thick accretion disk have been already extensively discussed in the literature, for both Kerr and non-Kerr spacetimes [2,4]. The theoretical framework is the Novikov–Thorne model [19]. The exact expression of the background metric enters the equations governing the time-averaged radial structure of the disk, the calculation of the propagation of the radiation from the disk to the distant observer, the motion of the particles of gas in the disk (determining the Doppler redshift and blueshift), and the inner edge of the disk, which is thought to be at the ISCO radius in the Novikov–Thorne model and eventually is the most important ingredient to infer the properties of the spacetime around the BH candidate.

The Novikov–Thorne model assumes that the disk is on the equatorial plane and that the disk's gas moves on nearly geodesic circular orbits. The time-averaged energy flux emitted from the surface of the disk is [19]

$$\mathcal{F}(r) = \frac{\dot{M}}{4\pi M^2} F(r), \tag{2}$$

where $F(r)$ is the dimensionless function

$$F(r) = -\frac{\partial_r \Omega}{(E-\Omega L)^2} \frac{M^2}{\sqrt{-G}} \int_{r_{\rm in}}^{r} (E-\Omega L)(\partial_\rho L)\, d\rho. \tag{3}$$

Here E, L, and Ω are, respectively, the conserved specific energy, the conserved axial-component of the specific angular momentum, and the angular velocity for equatorial circular geodesics; $G = -\alpha^2 g_{rr} g_{\phi\phi}$ is the determinant of the near equatorial plane metric, where $\alpha^2 = g_{t\phi}^2/g_{\phi\phi} - g_{tt}$ is the lapse function; $r_{\rm in}$ is the inner radius of the accretion disk, which is assumed to be the radius of the ISCO. Since the disk is in thermal equilibrium, the emission is blackbody-like and we can define an effective temperature $T_{\rm eff}(r)$ from the relation $\mathcal{F}(r) = \sigma T_{\rm eff}^4$, where σ is the Stefan–Boltzmann constant. The local specific intensity of the radiation emitted by the disk is

$$I_{\rm e}(\nu_{\rm e}) = \frac{2h\nu_{\rm e}^3}{f_{\rm col}^4} \frac{\Upsilon}{\exp(\frac{h\nu_{\rm e}}{k_{\rm B} T_{\rm col}}) - 1}, \tag{4}$$

where $T_{\rm col}(r) = f_{\rm col} T_{\rm eff}$ is the color temperature and $f_{\rm col}$ is the color factor, which takes non-thermal effects into account ($f_{\rm col} \approx 1.6$ in our case). $\nu_{\rm e}$ is the photon frequency, h is the Planck constant, $k_{\rm B}$ is the Boltzmann constant, and Υ is a function of the angle between the wavevector of the photon emitted by the disk and the normal of the disk surface, say ξ. The two most common options are $\Upsilon = 1$ (isotropic emission) and $\Upsilon = \frac{1}{2} + \frac{3}{4}\cos\xi$ (limb-darkened emission).

The spectrum can be conveniently written in terms of the photon flux number density as measured by a distant observer:

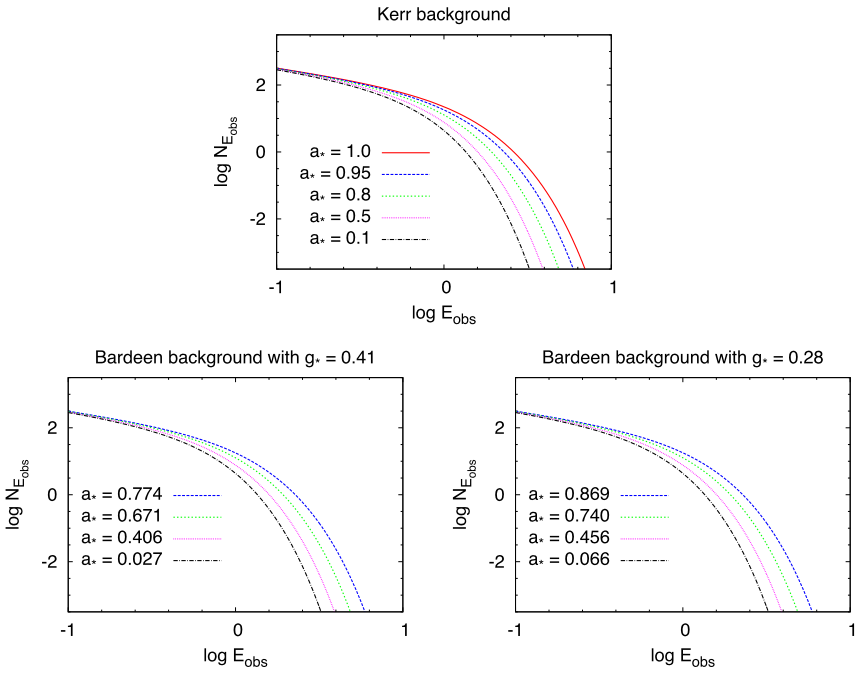

Fig. 2. Thermal spectra of thin accretion disks around a Kerr BH (top panel), a Bardeen BH with $g_* = 0.41$ (bottom right panel), a Bardeen BH with $g_* = 0.28$ (bottom left panel) for different values of the spin parameter a_*. The spectra on the bottom panels are extremely similar to the ones on the top panel with the same line style; that is, the spectrum of a Bardeen BH looks like the one of a Kerr BH with different spin. However, it is not always possible to mimic the spectrum of a very fast-rotating Kerr BH. For instance, a Bardeen BH with $g_* = 0.41$ cannot mimic a Kerr BH with $a_* = 1$, but only Kerr BHs with $a_* \lesssim 0.95$, because the maximum value of the spin parameter of a Bardeen BH with $g_* = 0.41$ is $a_* \approx 0.775$. See the text for more details.

$$
\begin{aligned}
N_{E_{\rm obs}} &= \frac{1}{E_{\rm obs}} \int I_{\rm obs}(\nu)\, d\Omega_{\rm obs} \\
&= \frac{1}{E_{\rm obs}} \int w^3 I_{\rm e}(\nu_{\rm e})\, d\Omega_{\rm obs} \\
&= A_1 \left(\frac{E_{\rm obs}}{\rm keV}\right)^2 \int \frac{1}{M^2} \frac{\Upsilon\, dX\, dY}{\exp[\frac{A_2}{g F^{1/4}} (\frac{E_{\rm obs}}{\rm keV})] - 1},
\end{aligned}
\tag{5}
$$

where $I_{\rm obs}$, $E_{\rm obs}$, and ν are, respectively, the specific intensity of the radiation, the photon energy, and the photon frequency measured by the distant observer. $I_{\rm e}(\nu_{\rm e})/\nu_{\rm e}^3 = I_{\rm obs}(\nu_{\rm obs})/\nu^3$ follows from the Liouville theorem. $d\Omega_{\rm obs} = dX\, dY/D^2$ is the element of the solid angle subtended by the image of the disk on the observer's sky, X and Y are the coordinates of the position of the photon on the sky, as seen by the distant observer, while D is the distance of the source. A_1 and A_2 are given by (reintroducing the constants $G_{\rm N}$ and c)

$$
\begin{aligned}
A_1 &= \frac{2({\rm keV})^2}{f_{\rm col}^4} \left(\frac{G_{\rm N} M}{c^3 h D}\right)^2 \\
&= \frac{0.07205}{f_{\rm col}^4} \left(\frac{M}{M_\odot}\right)^2 \left(\frac{\rm kpc}{D}\right)^2 \Upsilon\ {\rm keV}^{-1}\, {\rm cm}^{-2}\, {\rm s}^{-1},
\end{aligned}
$$

$$
\begin{aligned}
A_2 &= \left(\frac{\rm keV}{k_{\rm B} f_{\rm col}}\right) \left(\frac{G_{\rm N} M}{c^3}\right)^{1/2} \left(\frac{4\pi\sigma}{\dot{M}}\right)^{1/4} \\
&= \frac{0.1331}{f_{\rm col}} \left(\frac{10^{18}\, {\rm g\, s}^{-1}}{\dot{M}}\right)^{1/4} \left(\frac{M}{M_\odot}\right)^{1/2}.
\end{aligned}
\tag{6}
$$

w is the redshift factor and it turns out to be (for the details, see e.g. [4])

$$
w = \frac{\sqrt{-g_{tt} - 2 g_{t\phi}\Omega - g_{\phi\phi}\Omega^2}}{1 + \lambda\Omega},
\tag{7}
$$

where $\lambda = k_\phi/k_t$ is a constant of the motion along the photon path. Doppler boosting, gravitational redshift, and frame dragging are entirely encoded in the redshift factor w, while the effect of light bending enters the integral in Eq. (5), as every photon on the sky is associated with its emission point on the disk (this is done by integrating backward in time null geodesics from the observer to the disk).

In the Kerr spacetime, the model has five free parameters: the BH mass, M, the mass accretion rate, $\dot{M}$, the spin parameter, a_*, the disk inclination angle with respect to the line of sight of the distant observer, i, and the distance of the object, D. If M, i, and D can be estimated from independent measurements (e.g. optical observations), one can fit the X-ray data of the thermal spectrum of the disk and infer a_* and $\dot{M}$.[2] In the Bardeen metric, there is a sixth free parameter, g_*. However, as discussed above, the spectrum is somehow degenerate with respect a_* and g_*, in the sense that these two parameters cannot be determined independently, but it is only possible to infer a certain combination of them. In principle, the mass accretion rate $\dot{M}$ can be determined independently, from the low-energy part of the spectrum, whose photons are mainly emitted at large radii, where gravity is almost Newtonian. This is not really true in the case of X-ray data of stellar-mass BH candidates. However, in the case of good measurement it is a good approximation to assume that the determination of a_* (or a_* and g_*) is not correlated to the one of $\dot{M}$.

Results. We can now compare the thermal spectrum of thin disks around Kerr and Bardeen BHs to translate the bound of the spin parameter of the BH candidate in Cygnus X-1 found in Refs. [13,14] under the assumption of Kerr geometry into an allowed region

[2] Actually, for Cygnus X-1 the situation is more complicated and one has to fit also other features of the spectrum. However, the measurement of a_* is obtained from the properties of the thermal spectrum of the accretion disk [13,14].

on the spin parameter-deformation parameter plane of the Bardeen solution. We can make the calculation with the physical parameter of Cygnus X-1 ($M = 14.8 M_\odot$, $i = 27.1$ deg, $D = 1.86$ kpc, and even $\dot{M} = 1.3 \cdot 10^{17}$ g/s, which is roughly the mean mass accretion rate found from the data analyzed in [13,14]). However, the final result is quite independent of this choice, as in the end we compare Kerr and Bardeen spectra with the same model parameters except the ones providing the geometry of the spacetime. For more exotic metrics, this may not be true. For instance, a different Keplerian velocity and photon propagation may affect, respectively, the Doppler effect and the light bending, so the final constraint may depend on the disk's inclination angle i.

The 3σ-bound $a_* > 0.95$ found in [13] for the Kerr metric becomes the region inside the red solid line of Fig. 1 for the Bardeen background. The constraint is

$$a_* > 0.78, \qquad |g_*| < 0.41. \tag{8}$$

The 3σ-bound $a_* > 0.983$ found in [14] gives instead the region inside the blue dashed line of Fig. 1 and the bound is

$$a_* > 0.89, \qquad |g_*| < 0.28. \tag{9}$$

The region of objects without event horizon shown in Fig. 1 can be immediately ruled out for two reasons. First, like in the case of the Kerr metric with $g_* = 0$ [20], the thermal spectrum of disks around horizonless configurations is much harder, due to the sudden drop of the ISCO at smaller radii. Second, even if for $g_* \neq 0$ horizonless configurations can be created [21], they are expected to be highly unstable, due to the existence of the ergoregion and of stable orbits with negative energy [22].

Acknowledgements

This work was supported by the NSFC grant No. 11305038, the Innovation Program of Shanghai Municipal Education Commission grant No. 14ZZ001, the Thousand Young Talents Program, and Fudan University.

References

[1] C. Bambi, Mod. Phys. Lett. A 26 (2011) 2453, arXiv:1109.4256 [gr-qc];
C. Bambi, Astron. Rev. 8 (2013) 4, arXiv:1301.0361 [gr-qc].
[2] S.N. Zhang, W. Cui, W. Chen, Astrophys. J. 482 (1997) L155, arXiv:astro-ph/9704072;
L.-X. Li, E.R. Zimmerman, R. Narayan, J.E. McClintock, Astrophys. J. Suppl. 157 (2005) 335, arXiv:astro-ph/0411583;
J.E. McClintock, et al., Class. Quantum Gravity 28 (2011) 114009, arXiv:1101.0811 [astro-ph.HE].
[3] A.C. Fabian, M.J. Rees, L. Stella, N.E. White, Mon. Not. R. Astron. Soc. 238 (1989) 729;
A.C. Fabian, K. Iwasawa, C.S. Reynolds, A.J. Young, Publ. Astron. Soc. Pac. 112 (2000) 1145, arXiv:astro-ph/0004366;
C.S. Reynolds, M.A. Nowak, Phys. Rep. 377 (2003) 389, arXiv:astro-ph/0212065.
[4] C. Bambi, E. Barausse, Astrophys. J. 731 (2011) 121, arXiv:1012.2007 [gr-qc];
C. Bambi, Astrophys. J. 761 (2012) 174, arXiv:1210.5679 [gr-qc];
C. Bambi, Phys. Rev. D 87 (2013) 023007, arXiv:1211.2513 [gr-qc].
[5] D.F. Torres, Nucl. Phys. B 626 (2002) 377, arXiv:hep-ph/0201154;
T. Harko, Z. Kovacs, F.S.N. Lobo, Phys. Rev. D 80 (2009) 044021, arXiv:0907.1449 [gr-qc];
S. Chen, J. Jing, Phys. Lett. B 711 (2012) 81, arXiv:1110.3462 [gr-qc];
T. Johannsen, D. Psaltis, Astrophys. J. 773 (2013) 57, arXiv:1202.6069 [astro-ph.HE].
[6] C. Bambi, Phys. Rev. D 87 (2013) 084039, arXiv:1303.0624 [gr-qc];
P.S. Joshi, D. Malafarina, R. Narayan, Class. Quantum Gravity 31 (2014) 015002, arXiv:1304.7331 [gr-qc];
C. Bambi, D. Malafarina, Phys. Rev. D 88 (2013) 064022, arXiv:1307.2106 [gr-qc].
[7] C. Bambi, J. Cosmol. Astropart. Phys. 1308 (2013) 055, arXiv:1305.5409 [gr-qc].
[8] C. Bambi, J. Cosmol. Astropart. Phys. 1209 (2012) 014, arXiv:1205.6348 [gr-qc];
C. Bambi, arXiv:1312.2228 [gr-qc].
[9] H. Krawczynski, Astrophys. J. 754 (2012) 133, arXiv:1205.7063 [gr-qc].
[10] C. Bambi, Phys. Rev. D 85 (2012) 043002, arXiv:1201.1638 [gr-qc];
C. Bambi, Phys. Rev. D 86 (2012) 123013, arXiv:1204.6395 [gr-qc].
[11] Z. Li, C. Bambi, J. Cosmol. Astropart. Phys. (2014), in press, arXiv:1309.1606 [gr-qc];
Z. Li, L. Kong, C. Bambi, arXiv:1401.1282 [gr-qc].
[12] J.E. McClintock, et al., Astrophys. J. 652 (2006) 518, arXiv:astro-ph/0606076.
[13] L. Gou, et al., Astrophys. J. 742 (2011) 85, arXiv:1106.3690 [astro-ph.HE].
[14] L. Gou, et al., arXiv:1308.4760 [astro-ph.HE].
[15] J.L. Blum, et al., Astrophys. J. 706 (2009) 60, arXiv:0909.5383 [astro-ph.HE];
R. Duro, et al., Astron. Astrophys. 533 (2011) L3, arXiv:1108.1157 [astro-ph.HE];
A.C. Fabian, et al., Mon. Not. R. Astron. Soc. 424 (2012) 217;
J.A. Tomsick, et al., Astrophys. J. 780 (2014) 78, arXiv:1310.3830 [astro-ph.HE].
[16] J.M. Miller, C.S. Reynolds, A.C. Fabian, G. Miniutti, L.C. Gallo, Astrophys. J. 697 (2009) 900, arXiv:0902.2840 [astro-ph.HE].
[17] E. Ayon-Beato, A. Garcia, Phys. Lett. B 493 (2000) 149, arXiv:gr-qc/0009077.
[18] C. Bambi, L. Modesto, Phys. Lett. B 721 (2013) 329, arXiv:1302.6075 [gr-qc].
[19] I.D. Novikov, K.S. Thorne, Astrophysics of black holes, in: C. De Witt, B. De Witt (Eds.), Black Holes, Gordon and Breach, New York, 1973, pp. 343–450;
D.N. Page, K.S. Thorne, Astrophys. J. 191 (1974) 499.
[20] R. Takahashi, T. Harada, Class. Quantum Gravity 27 (2010) 075003, arXiv:1002.0421 [astro-ph.HE].
[21] Z. Li, C. Bambi, Phys. Rev. D 87 (2013) 124022, arXiv:1304.6592 [gr-qc].
[22] P. Pani, E. Barausse, E. Berti, V. Cardoso, Phys. Rev. D 82 (2010) 044009, arXiv:1006.1863 [gr-qc].